Optical heterodyne imaging and Wigner phase space distributions

A. Wax and J. E. Thomas

Department of Physics, Duke University, Durham, North Carolina 27708-0305

Received May 6, 1996

We demonstrate that optical heterodyne imaging directly measures smoothed Wigner phase space distributions. This method may be broadly applicable to fundamental studies of light propagation and tomographic imaging. Basic physical properties of Wigner distributions are illustrated by experimental measurements. © 1996 Optical Society of America

In 1932 Wigner[1] introduced a wave-mechanical phase space distribution function that plays a role closely analogous to that of a classical phase space distribution in position and momentum. For a wave field varying in one spatial dimension, $\mathcal{E}(x)$, the Wigner phase space distribution is given by[2]

$$W(x,\,p) = \int \frac{\mathrm{d}\epsilon}{2\pi} \exp(i\epsilon p)\langle \mathcal{E}^*(x + \epsilon/2)\mathcal{E}(x - \epsilon/2)\rangle\,, \tag{1}$$

where x is the position, p is a wave vector (momentum), and angle brackets denote a statistical average. Despite their frequent use in theory and potential practical importance to imaging,[3–5] Wigner phase space distributions have received relatively little attention in optical measurements. Because rigorous transport equations can be derived for Wigner distributions, these distributions are important for fundamental studies of light propagation and tomographic imaging.

In this Letter we demonstrate that the mean-square heterodyne beat signal, which we measure in real time, is proportional to the overlap of the Wigner phase space distributions for the local oscillator and signal fields. This remarkable result, which seems not to have been exploited previously in heterodyne detection,[6,7] permits us to measure Wigner phase space distributions for the signal field directly as contour plots with high dynamic range. The measured phase space contours are smoothed Wigner distributions for the signal field; i.e., the phase space resolution is determined by the diffraction angle and the spatial width of the local oscillator.[8] We measure Wigner distributions for cases that illustrate their basic physical properties.

The scheme of the heterodyne method, Fig. 1, employs a helium–neon laser beam that is split at BS1 into a 1-mW local oscillator (LO) and a 1-mW signal beam. One can introduce a sample into the signal path to study the transmitted field. The signal beam is mixed with the LO at a 50–50 beam splitter (BS2). Technical noise is suppressed by use of a standard balanced detection system.[9] The beat signal at 10 MHz is measured with an analog spectrum analyzer. An important feature of the experiments is that the analog output of the spectrum analyzer is squared by a low-noise multiplier.[10] The multiplier output is fed to a lock-in amplifier, which subtracts the mean-square signal and noise voltages with the input beam on and off.[11] In this way the mean-square electronic noise and the LO shot noise are subtracted in real time, and the lock-in output is directly proportional to the mean-square beat amplitude $\langle |V_B|^2\rangle$.

The beat amplitude V_B is determined in the paraxial ray approximation by the spatial overlap of the LO and signal fields in the detector planes, $z = z_D$.[6] The fields in the detector planes can be related to the fields in the source planes at input lenses L1 and L2 ($z = 0$), which have equal focal lengths f. L2 is translated off axis by a distance d_p, and mirror M1 is translated off axis a distance d_x. The mean-square beat amplitude is obtained in the Fresnel approximation as

$$\begin{aligned}\langle |V_B|^2\rangle &\propto \left\langle \left| \int \mathrm{d}x' \mathcal{E}_{\mathrm{LO}}^*(x',\, z_D)\mathcal{E}_S(x',\, z_D) \right|^2 \right\rangle \\ &= \left\langle \left| \int \mathrm{d}x \mathcal{E}_{\mathrm{LO}}^*(x - d_x,\, z = 0)\mathcal{E}_S(x,\, z = 0) \right.\right. \\ &\qquad \left.\left. \times \exp\!\left(ik\frac{d_p}{f}x\right) \right|^2 \right\rangle. \end{aligned} \tag{2}$$

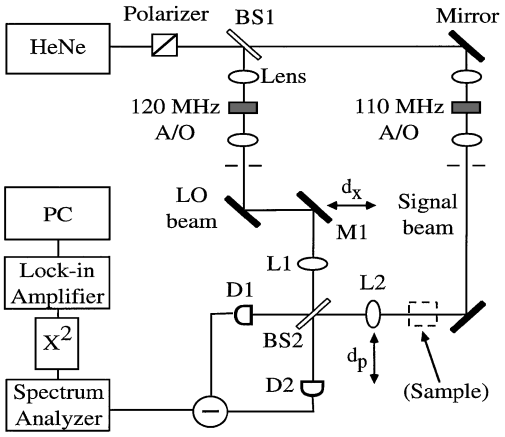

Fig. 1. Scheme for heterodyne measurement of Wigner phase space distributions. The displacement d_x of mirror M1 determines the position x, and the displacement d_p of lens L2 determines the momentum p. A/O's, acousto-optic modulators.

0146-9592/96/181427-03$10.00/0

Here $\mathcal{E}$ is a slowly varying field amplitude (band center frequency phase factor removed) and $k = 2\pi/\lambda$. For simplicity the corresponding y integral in the detector plane is suppressed. It is assumed here that the Rayleigh and coherence lengths of the LO field are large compared with d_x, so the translation of M1 simply shifts the center of the input LO field without significantly altering the LO optical path length before L1. When this is not the case, a variable LO path length can be introduced to compensate for the path-length change that is due to moving M1. The detectors, D1 and D2, are located in the Fourier planes $z_D = f$ of both lenses L1 and L2, so the LO position in the detector planes remains fixed as d_x is scanned.

Using Eq. (1), we can rewrite relation (2) (suppressing the y integration) as

$$\langle |V_B(d_x, d_p)|^2 \rangle \propto \int \mathrm{d}x\mathrm{d}p\, W_{\mathrm{LO}}(x - d_x, p + kd_p/f) W_S(x, p). \quad (3)$$

$W_S(x, p)$ [$W_{\mathrm{LO}}(x, p)$] is the Wigner distribution of the signal (LO) field in the plane of L2 (L1) given by Eq. (1). Relation (3) shows that the mean-square beat signal yields a phase space contour plot of $W_S(x, p)$ with phase space resolution determined by W_{LO}.[8] The current system measures position over ± 1 cm and momentum over $\pm 0.1\, k$ (i.e., ± 100 mrad).

First we review the basic properties of Wigner distributions for Gaussian signal beams and demonstrate their measurement as phase space contours. A Gaussian beam has a slowly varying field of the form $\mathcal{E}(x) \propto \exp[-x^2/(2w^2) + ikx^2/(2R)]$. Equation (1) yields the corresponding Wigner distribution (normalized to unity):

$$W(x, p) = (1/\pi)\exp(-x^2/w^2) \times \exp\left[-w^2(p - kx/R)^2\right]. \quad (4)$$

Here the intensity $1/e$ width is w and the wave-front radius of curvature is R.

Wigner distributions obey a simple propagation law in free space: The convective derivative is zero, which follows from the wave equation in the slowly varying amplitude approximation. For a time-independent Wigner distribution propagating paraxially in the **z** direction with wave vector $p_z \simeq k$ the distribution in the plane $z = L$ then is given in terms of that for $z = 0$ according to $W(x, p, z = L) = W(x - pL/k, p, z = 0)$. Hence the x argument propagates in straight lines. For propagation through a lens of focal length f it is easy to show that the quadratically varying phase of the lens, $\phi(x) = -kx^2/2f$, leads to a change in the momentum argument: $p \rightarrow p + kx/f$. These results easily yield the *ABCD* law of Gaussian beam optics.[12] Hence, for example, suppose that W_G is the Wigner distribution for a Gaussian beam at a waist, i.e., Eq. (4), with $w = a$ and $R = \infty$. Then it is easy to show that $W(x, p, z = L) = W_G(x - pL/k, p)$ takes the form of Eq. (4), with w and R given by the usual Gaussian beam results that properly include diffraction.[12]

In the experiments we begin with Gaussian signal fields, and $W_S(x, p)$ takes the form of Eq. (4). The LO beam is chosen to be Gaussian with its waist in the plane of L1. Then $W_{\mathrm{LO}}(x, p) = W_G(x, p)$ is given by Eq. (4) with $w = a = 380\ \mu$m and $R = \infty$. With the sample removed (Fig. 1), the signal beam waist and radius of curvature are determined by a lens (not shown) that focuses the input beam to a waist, $a_s = 35\ \mu$m, at a plane located a distance L behind the signal input plane at L2.

Figure 2 shows measured phase space contours, $\langle |V_B(d_x, d_p)|^2 \rangle$, obtained by scanning d_x and d_p with stepper motors. The position axis denotes the LO center position d_x. The momentum axis denotes the LO center momentum p_c in units of the optical wave vector: $p_c/k = -d_p/f$. The contours rotate as the distance L is changed. For $L = 0$ the waist is at L2 and the curvature $R = \infty$. The phase space ellipse has its principal axes oriented vertically and horizontally. The position width of the distribution is dominated by the LO width in this case, and the momentum width is dominated by the signal beam. The phase space ellipse rotates clockwise (counterclockwise) for $L = 5$ cm ($L = -5$ cm), indicating positive (negative) curvature, i.e., $R > 0$ ($R < 0$) at L2. The rotation of the phase space ellipse is a simple consequence of the correlation between the momentum and the position for a beam with curvature, Eq. (4). As one would expect for a diverging beam, the mean momentum shifts to the right for $x > 0$. These results clearly demonstrate how the measured phase space contours are sensitive to the spatially varying phase of the field.

It is instructive to measure phase space contours for a source consisting of two mutually coherent, spatially separated Gaussian beams. The input beams are

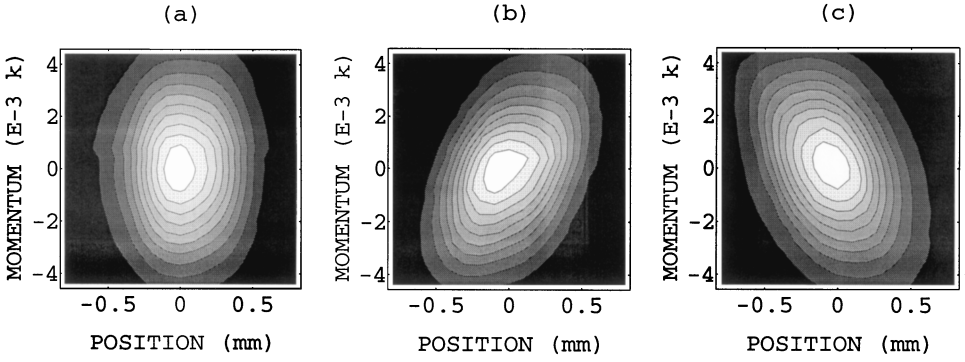

Fig. 2. Measured Wigner phase space contours for Gaussian signal beams: (a) beam waist (flat wave front), (b) diverging (positive wave-front curvature), (c) converging (negative wave-front curvature).

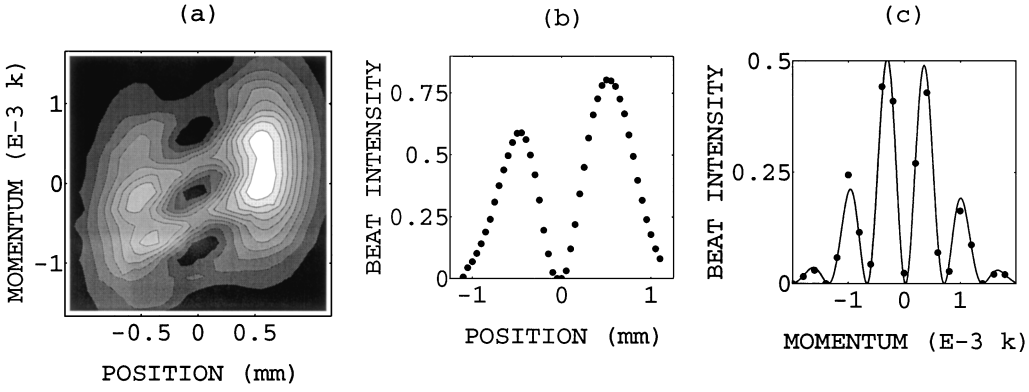

Fig. 3. Measured Wigner phase space contours for two spatially separated, mutually coherent beams: (a) Phase space contour, (b) position profile for momentum $p = 0$, (c) momentum profile at position $x = 0$. Dotted curves, data; solid curve, theory.

centered at positions $x = \pm d/2$ with $d = 1$ mm and intensity $1/e$ radii $a_s = 110$ μm at the waist in the plane of L2. The Wigner distribution for this signal field is given by Eq. (1) as

$$W_S(x, p) = W_G(x - d/2, p) + W_G(x + d/2, p) + 2W_G(x, p)\cos(dp + \varphi), \quad (5)$$

where W_G denotes the Wigner distribution for either Gaussian beam at its waist. An interesting feature of this distribution is that for $d \gg a_s$, as used here, the cosine term is dominant at $x = 0$ and negative values are obtained as p is varied.

Figure 3 shows the measured contour plots. In the central region the intensity oscillates with nearly 100% modulation but is positive definite, as it must be.[8] Note that the orientation of the phase space ellipses indicates beam waists. The right-hand ellipse is centered at a higher momentum than the left, indicating a small angle between the two input beams. The two-peaked position profile for $p = 0$ is shown along with the oscillatory momentum profile for $x = 0$ midway between the two intensity peaks. The solid curve shows the theoretical fit to the momentum distribution, with a signal beam $1/e$ width of 103 μm, which is consistent with diode array measurements within 10%.

In conclusion, we have demonstrated direct heterodyne measurement of smoothed Wigner phase space distributions. This method achieves high dynamic range[13] and is applicable to light from arbitrary samples. Study of Wigner distributions may be useful for placing biological imaging methods, such as optical coherence tomography[14] and potential high-resolution optical biopsy techniques, on a rigorous theoretical footing.

This research was supported by the U.S. Air Force Office of Scientific Research and the National Science Foundation. We are indebted to M. G. Raymer for many stimulating conversations regarding it and to S. John for a preprint of his paper.

References

1. E. P. Wigner, Phys. Rev. Lett. **40,** 749 (1932).
2. M. Hillery, R. F. O'Connel, M. O. Scully, and E. P. Wigner, Phys. Rep. **106,** 121 (1984).
3. D. F. McAlister, M. Beck, L. Clarke, A. Mayer, and M. G. Raymer, Opt. Lett. **20,** 1181 (1995).
4. M. G. Raymer, C. Cheng, D. M. Toloudis, M. Anderson, and M. Beck, in *Advances in Optical Imaging and Photon Migration* (Optical Society of America, Washington, D.C., 1996), pp. 236–238.
5. S. John, G. Pang, and Y. Yang, Proc. SPIE **2389,** 64 (1995).
6. See, for example, V. J. Corcoran, J. Appl. Phys. **36,** 1819 (1965); A. E. Siegman, Appl. Opt. **5,** 1588 (1966); S. Cohen, Appl. Opt. **14,** 1953 (1975); A. Migdall, B. Roop, Y. C. Zheng, J. E. Hardis, and G. J. Xia, Appl. Opt. **29,** 5136 (1990).
7. Recent heterodyne studies in turbid media include K. P. Chan, M. Yamada, B. Devaraj, and H. Inaba, Opt. Lett. **20,** 492 (1995); M. Toida, M. Kondo, T. Ichimura, and H. Inaba, Appl. Phys. B **52,** 391 (1991).
8. The mean-square beat is positive definite and takes the form of a smoothed Wigner distribution. See N. D. Cartwright, Physica **83A,** 210 (1976).
9. H. P. Yuen and V. W. S. Chan, Opt. Lett. **8,** 177 (1983).
10. This method has been used in light beating spectroscopy; see H. Z. Cummins and H. L. Swinney, in *Progress in Optics*, E. Wolf, ed. (North-Holland, New York, 1970), Vol. VIII, Chap. 3, pp. 133–200.
11. This method has been used by G. L. Abbas, V. W. S. Chan, and T. K. Yee, IEEE J. Lightwave Technol. **3,** 1110 (1985).
12. A. Yariv, *Introduction to Optical Electronics* (Holt, Rinehart, & Winston, New York, 1976), Chap. 3, p. 35.
13. A. Wax and J. E. Thomas, in *Advances in Optical Imaging and Photon Migration* (Optical Society of America, Washington, D.C., 1996), pp. 238–242.
14. The magnitude of the mean beat amplitude (rather than the mean square) is usually measured in this case. See, for example, J. A. Izatt, H. R. Hee, G. M. Owen, E. A. Swanson, and J. G. Fujimoto, Opt. Lett. **19,** 590 (1994).